

## **Geophysical investigations on the contribution of irrigation channels to landslide activity in Tusion, Tajikistan**

**Gisela Domej<sup>1\*</sup>, Umed Aslanov<sup>2</sup> and Anatoly Ischuk<sup>3</sup>**

<sup>1</sup>*IFSTTAR – GERS – Sols, Roches et Ouvrages Géotechniques – 14-20 Boulevard Newton – 77447 Marne-la-Vallée, France*

<sup>2</sup>*Hilfswerk International – Bokhtar Street 37 – 734000 Dushanbe, Tajikistan*

<sup>3</sup>*Academy of Sciences of the Republic of Tajikistan – IGEES – Ayni Street 267 – 734063 Dushanbe, Tajikistan*

*\*E-Mail address of the corresponding author: g.domej@gmail.com*

*Submitted: Aug. 26, 2019 / Accepted: Oct. 20, 2019 / Published online: Nov. 29, 2019*

### **Abstract**

Post-glacial geomorphological settings bearing vast amounts of colluvium as well as alluvial and moraine deposits are typical features in high mountainous environments such as the Himalayas, the Hindu Kush, the Pamir, the Karakoram and the Tien Shan. Due to a lack of alternative living space in narrow valleys, agglomerations are often located on these unstable grounds and regularly experience displacements across the ground surface and subsequent damage to building stock and infrastructure.

Hosting two post-glacial landslide deposits and one gravitational creep within its inhabited areas, the village of Tusion, South-Western Tajikistan, was chosen to conduct geophysical surveys with the aim to determine the geomorphological causes of regularly experienced slope deformations with a particular interest in the contribution of non-isolated irrigation channels crossing the mountain flanks. Over the last two decades, uncontrolled seepage from a network of small-scale irrigation channels is believed to be responsible for water infiltration to deeper horizons and – thereby – reactivate ancient sliding surfaces within the two landslide deposit zones. Also, the gravitational creep in one village part seems to be likewise triggered.

Using refraction seismics and Schlumberger geoelectrics, stratigraphic structures, properties of involved rock material and saturation patterns were assessed in order to provide complementary information about the underground of concerned slopes to a previously conducted hazard assessment by separate Non-Governmental Organizations. Results of the geophysical surveys show conclusive correlations with the hazard maps and local damage reports straining that one of the major destabilizing factors for all concerned slopes consists of uncontrolled water dissipation to the underground.

*Keywords:* post-glacial landslide, gravitational creep, refraction seismics, geoelectrics, water infiltration, irrigation channels

### **1. Introduction**

About 15 km south-east of Khorog, the local capital of the Gorno-Badakhshan Autonomous Region (GBAO), Tajikistan, the village of Tusion (37°21'42.6"N, 71°39'50.3"E; Fig. 1a) is located in a 4<sup>th</sup> order side-valley (Hack, 1957) to the Panj

River that forms the border between Tajikistan and Afghanistan. Similar to many other small-scale agglomerations in the region, the village is subjected to a system of active landslides entailing regular slope movements and damage to infrastructure (Fig. 1b). This geomorphological setting is typical for post-glacial landscapes that

nowadays characterize the Western Pamir with its deeply incised valleys between high peaks, sharp mountain flanks and vast alluvial and colluvial deposits (Kreutzmann, 2011a).

The geological setting of the Roshtqala Range around Tusion – and generally the Western Pamir – consists of a Precambrian crystalline and metamorphic basement showing regional migmatization as well as plutonic intrusions. On top of this base lie Upper-Paleozoic sedimentary series (Brookfield, 2000; Karapetov et al., 1975; Slavin, 1976). Regardless of the petrology, rock material close to the ground surface is clastic and disconnected displaying vast amounts of quaternary deposits resulting from glacial and post-glacial degradation processes and weathering. With time, these processes created highly favorable conditions for landslides and other types of mass movements, which nowadays represent one of the most significant threats in the region. Due to reasons of accessibility, the principal agglomerations in GBAO usually are situated in erosion-dominated locations such as narrow valley floors, alluvial fans and unstable slopes and are, hence, widely affected by slope deformation.

Alongside floods and avalanches, earthquakes are to be considered as a major threat – and frequently cause consecutive landslides. Disposing of an extraordinary thick crust of up to 80 km, the Pamir Mountains are heavily faulted and regularly experience earthquakes with deep hypocenters and magnitudes up to 7 on the Richter Scale (Kordonskaya & Shebalin, 1977; Searle, 2008).

### *1.1. Site conditions in Tusion*

The prevalent site conditions in Tusion reflect well the above mentioned geological, geodynamical and geomorphological settings of the region. The climate is extremely arid; low precipitation rates cause pastureland to be sparse and small-scale agriculture as well as livestock farming are

significantly dependent on a network of man-made irrigation channels providing freshwater from remote glacial catchments (Breckle & Kleinn, 2011; Kreutzmann, 2011b). Besides climatic factors, these hostile living conditions are owed to loose and unconsolidated grounds that bear an abundance of features linked to glacial and post-glacial erosion as well as to glacial retreat. Side and base moraines testify to scouring of the valley flanks during the last Pleistocene glaciation; also, local ice-polished topographic elevations can be considered as evidence of ice mass migration. The most prominent post-glacial features are two large landslides and one gravitational creep.

The two landslides (village parts Delokh and Shosh; Fig. 1b, Tab. 1) are believed to be a result of slope instability due to the lack of supporting ice masses after the glacial retreat and subsequent exposition of the slopes to insulation, precipitation and permafrost degradation. A strong earthquake could also have played a role during the triggering process (Strom & Abdrakhmatov, 2018). In both concerned village parts gradual displacements as well as sudden ruptures, ground sagging, local patterns of solifluction and shallow creeps regularly cause damage to buildings and infrastructure such as roads, footpaths and irrigation channels (Fig. 2a-b, Fig. 3a-c). Both landslides dispose of delimited deposit zones that stand out from the surrounding topography; however, only the bigger Delokh Landslide is assumed to have created a natural barrier lake during the past before having been incised by the Sharfdara River again. Today the landslide deposit is gradually undercut by the river causing the toe to become steeper and favoring further landslide activity.

The gravitational creep in the village part of Lakhshik (Fig. 1b, Fig. 2b, Tab. 1) appears to be different, as it does not show a distinct deposit area, although the slope experiences the same geomorphological features of displacement as the other two concerned

slopes. Here, one theory is that – as the ice masses had moved towards valley outlet in the north – they had polished and exerted stabilizing pressure on the nowadays inhabited flank of the topographic elevation. This assumption is emphasized by the fact that the northern side of the polished hilltop is much more fissured and coarse what often happens when ice freezes in low-pressure zones behind an elevation and eventually rips off rocks during ice migration. The preferred settlement took then place on the smoother side of the hilltop. As it is the most populous village part of Tusion, land-use is most significant what might contribute to the creeping activity.

### 1.2. Objectives of the geophysical surveys

Being part of an internationally funded NGO-project aiming for “ready-to-use” solutions, the main objective of the

geophysical surveys was to provide a high-resolution insight into the underground of the three concerned slopes in order to explain the regularly experienced damage throughout the settlements and to evaluate the hazard potential.

From testimonies of the local inhabitants, ground displacements reaching as deep as several meters are witnessed since the area was inhabited in the 1990s (FOCUS et al., 2009). Accounting for the apparent coincidence of settlement and ground movement, refraction seismics and geoelectrics seemed suitable tools. On the one hand, arrays of several tens of meters allow for depth information that covers the uppermost horizons through which displacements are witnessed. On the other hand, geoelectrics are particularly sensitive to water contents, which, in return, are often linked to land use and settlement patterns.

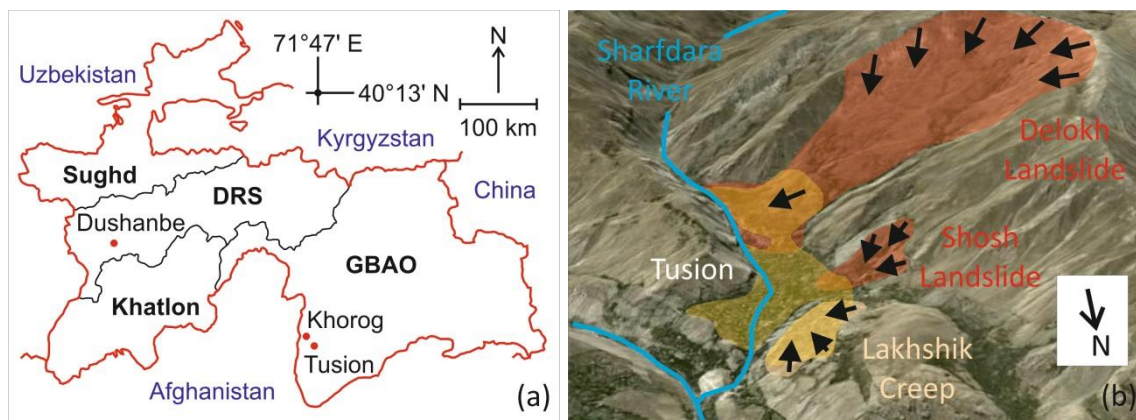


Fig. 1a-b. Location of Tusion within Tajikistan (a) and the three village parts with respective sliding processes (b). GBAO stands for Gorno-Badakhshan Autonomous Region, DRS for the District of Republican Subordination. Yellow shading refers to inhabited areas.

Tab. 1. Landslide locations and dimensions in different settlement zones.

Village part	Coordinates	Elevations and maximum landslide dimensions	Settlements
Delokh	37°21'29.2"N, 71°39'48.2"E	elevation: 4000-2800 masl length: 1000 m width: 4000 m	on landslide deposit zone
Shosh	37°22'02.9"N, 71°39'33.6"E	elevation: 3000-2700 masl length: 400 m width: 700 m	on landslide deposit zone
Lakhshik	37°22'36.7"N, 71°39'38.2"E	elevation: 2700-2600 masl length: unclear width: unclear	all across creep zone



Fig. 2a-b. Deposit zone of the Delokh Landslide (a) with secondary slides (yellow) and soil creeps (beige); gravitational creep (b) of Lakhshik with the polished hilltop flank in the back above the settlements. The Shosh Landslide is shown partly behind a mountain flank (b).

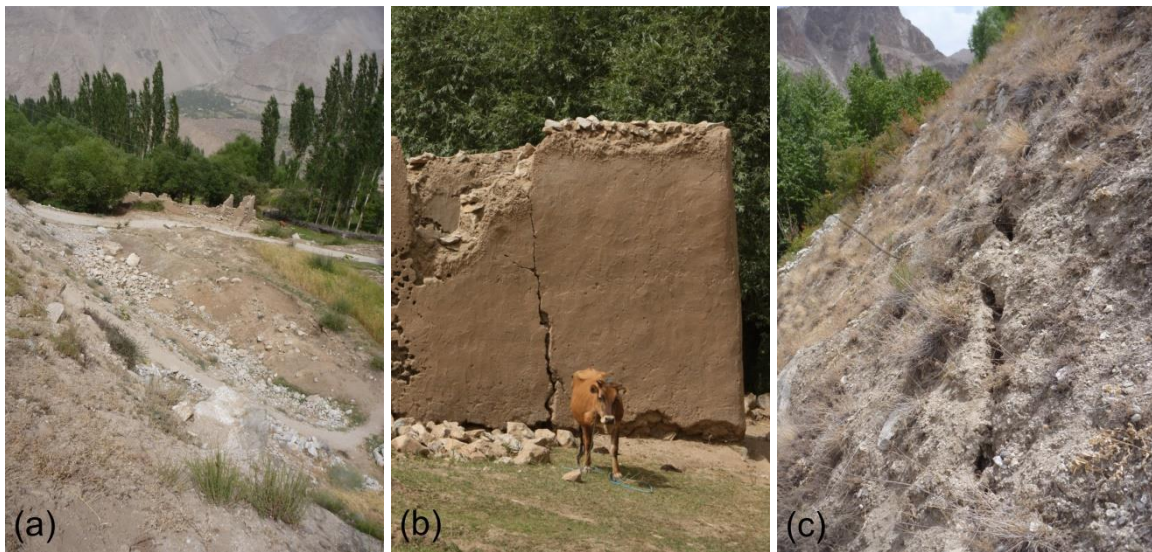


Fig. 3a-c. Secondary slides (a), damaged building stock (b) and ground cracks of 10-20 cm (c) in Delokh. The remnants of the wall (b) serve as a benchmark for the first picture (a).

## 2. Methodology

Being flexible, easily portable even in difficult terrain, non-invasive and relatively cost-efficient, refraction seismics and geoelectrics are – especially in combination – useful methods for shallow subsurface analysis (Bichler et al., 2004; Konagai et al., 2005). By the estimation of shear wave velocity distributions, refraction seismics assess structures of sediment cover and the underlying bedrock, whereas geoelectrics allow for stratigraphic mapping including aquifer localization via conductivity patterns. Particularly with respect to landslides, authors showed over the last decades that failure surfaces as well as lateral extents of landslides can be successfully delineated using refraction seismics and geoelectrics (Bogoslovsky &

Ogilvy, 1977; Brooke, 1973; Cummings & Clark, 1988; Glade et al., 2005; Hack, 2000; Havenith et al., 2000 & 2018; Jongmans & Garambois, 2007; Singh et al., 2012); Mauritsch et al. (2000) also used geoelectrics for deep-seated creeps.

### 2.1. Application of the geophysical methods in Tusion

Geophysical surveys were carried out in the three village parts of Tusion; however, no refraction seismics were performed in Shosh. Usually, arrays followed roads and footpaths or crossed straight fields, meadowlands or non-vegetated slopes to avoid inflections. As for the nomenclature, each array bears a three-letter code followed by the array number per location: the first letter indicates the village part (Delokh / Lakhshik / Shosh), the second refers to the

method (refraction seismics / geoelectrics) and the third notes the orientation (horizontal with respect to the altimetry / along the slope). Both array types were set up with a parallel offset of approximately 10 m and lengthwise overlap each other (Fig. 4, Fig. 6, Fig. 9, Fig. 10, Tab. 2, Tab. 3).

Separate refraction seismic arrays consist of 24 cable-linked geophones with a spacing of either 5.0 m or 2.5 m. The seismic source was provided by a sledgehammer striking a hard rubber plate at five locations: two offset strokes at a straight extension of 20 m from the array extremities, two onset strokes at the first and the last geophone and one onset stroke at the array center. In order to minimize the signal-to-noise-ratio, five strokes were automatically stacked for each location by a GEOMETRIX ES-3000 seismograph and monitored by a field computer. In the aftermath, data were processed using the INTERPEX (2008a) software IXRefraX. By inverse data

modeling, two-layer refraction models were established over the first tens of meters of depth, taking into account the local topography alongside the arrays that were tracked with a portable GPS-device.

Individual geoelectrics arrays were set up according to the Schlumberger Geometry with two stationary potential electrodes around the array center and two mobile induction electrodes being symmetrically displaced outwards to distances of two times 80-300 m. Resistivities were measured with a multi-meter station applying direct current with reversed directions in intervals of 10 Hz in order to avoid polarization effects. Obtained depth soundings are representative for the array center points assuming homogeneous and isotropic soil properties. Geoelectrics data were processed with the INTERPEX (2008b) software IX1D creating multi-layer models as resistivity soundings reach deeper horizons than the refraction seismics profiles.

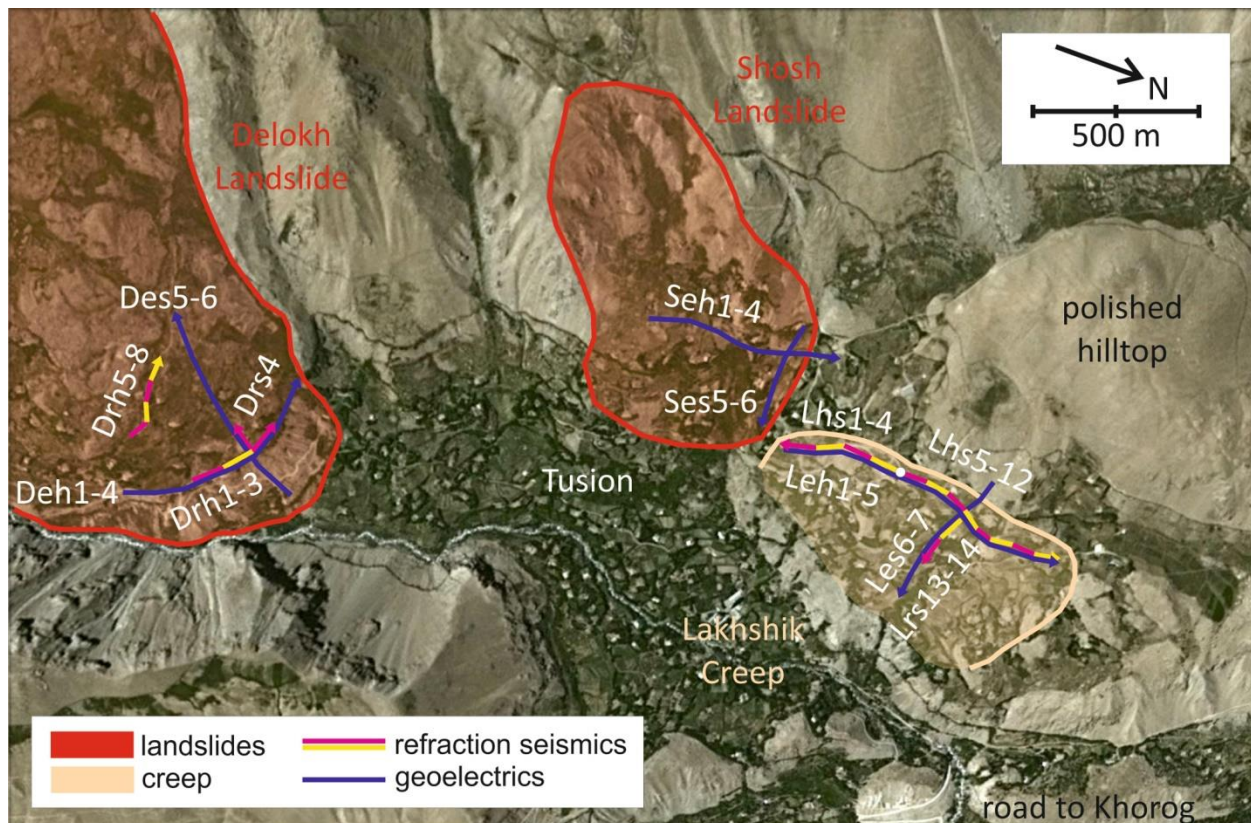
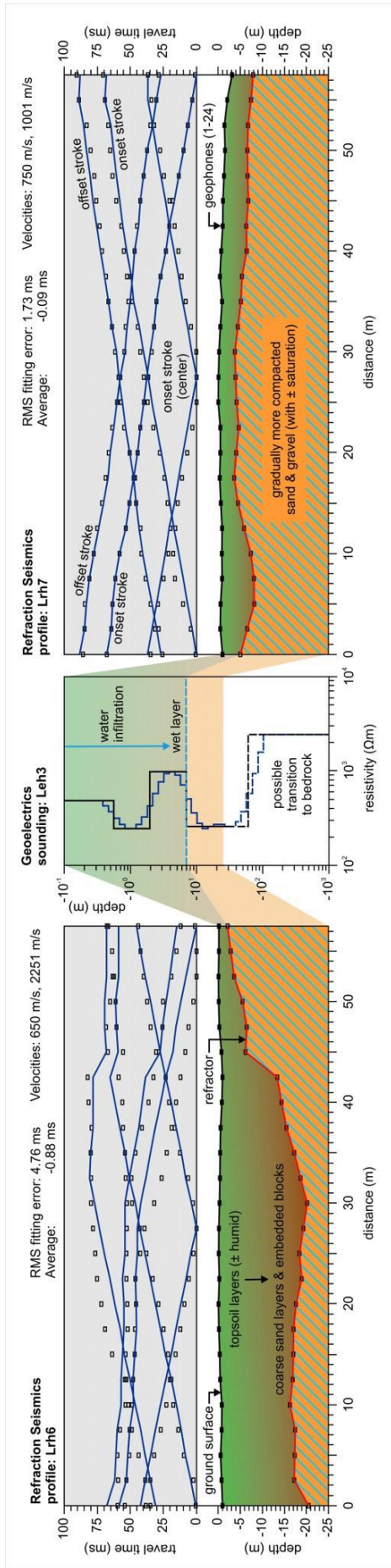


Fig. 4. Layouts of the refraction seismics and geoelectrics arrays in the three village parts (Google Earth, 2012).



← Fig. 5. Overlap of the refraction seismic profiles Lrh6-7 with the geoelectric sounding LeH3. Colors are as indicated in Fig. 9.

### 3. Results of the refraction seismics and geoelectrics surveys

In the following, results from the refraction seismics and the geoelectrics surveys are brought together and visualized in integrated transversal cross-sections (TCS); as an example of such a combination, Fig. 5 shows the overlap of the refraction seismics profiles Lrh6-7 with the geoelectric sounding LeH3 in Lakhshik. The longitudinal cross-sections (LCS) in the direction of the respective slopes appeared to be very homogeneous with almost slope-parallel layer sequences and are, therefore, not shown. Since the aim of the geophysical surveys was not to scrutinize the actual rock materials, but rather to distinguish relevant horizons that explain the permanent movements of the concerned slopes, interpretations are based on a simple classification of material within the shallow and deep underground as mentioned in the legend in Fig. 9. A distinction is made between significantly heterogeneous topsoil layers on the first meters, an almost omnipresent coarse layer with embedded blocks, gradually more compacted sand and gravel horizons and finally hard and compacted material with a probable transition to bedrock. It is important to note that depths of main boundaries that are assumed to form sliding surfaces are shown as a compromise between the results of both geophysical methods (Fig. 6, Fig. 9 and Fig. 10). Refraction seismics allow refractor location in 2D and, thus, give a range of depths throughout a distinct profile (Tab. 2), whereas geoelectrics provide depth soundings in 1D without lateral variation of detected layer boundaries (Tab. 3).

#### 3.1. Delokh

In Delokh, refraction seismics were carried out across the settlement area and on the plateau formed by the landslide deposit (Fig. 4). In the two locations, both methods

delivered very similar results. At the lower site (Drh1-3, Drs4) the two-layer model revealed a clear refractor in depths around 6-9 m from the ground surface at which shear wave velocities increase from 400-600 m/s to 750-1150 m/s (Tab. 2) indicating the transition from loose and unconsolidated to more compact material. Single value refractor depths are due to flat refractors as proposed by the model; otherwise, depths are variable on some meters of range. Like the refraction seismic arrays Drh1-3, also array Drs4 across the slope shows variable refractor depths; however, shallower depths appear at the array extremities, and the major part of the profile displays refractor depths of 18 m below the ground surface. Results from the upper site (Drh5-8) are consistent in terms of shear wave velocities and refractor depths. At 8-18 m from the ground surface, shear wave velocities increase from 400-550 m/s to 950-1500 m/s.

Generally, separate arrays connect well to each other; the fact that refractors are located slightly deeper in the upper part of Delokh seems coherent with the array Drs4 that reports slightly greater depths reaching from the scarp up towards the plateau.

The most prominent feature that consistently appears throughout the individual geoelectric soundings in Delokh (Deh1-4) is one distinct change of resistivity in around 3-15 m from the ground surface (Tab. 3). While the multi-layer models propose between four and six layer boundaries, only those in the mentioned depth show abrupt transitions from 2500-4000  $\Omega\text{m}$  to 200-800  $\Omega\text{m}$  testifying to a higher conductivity – and hence water saturation – at and below this relevant layer boundary. Models of the two profiles in the direction of the slope (Des5-6) suggest the same resistivity ranges at a slightly deeper layer boundary at 25 m.

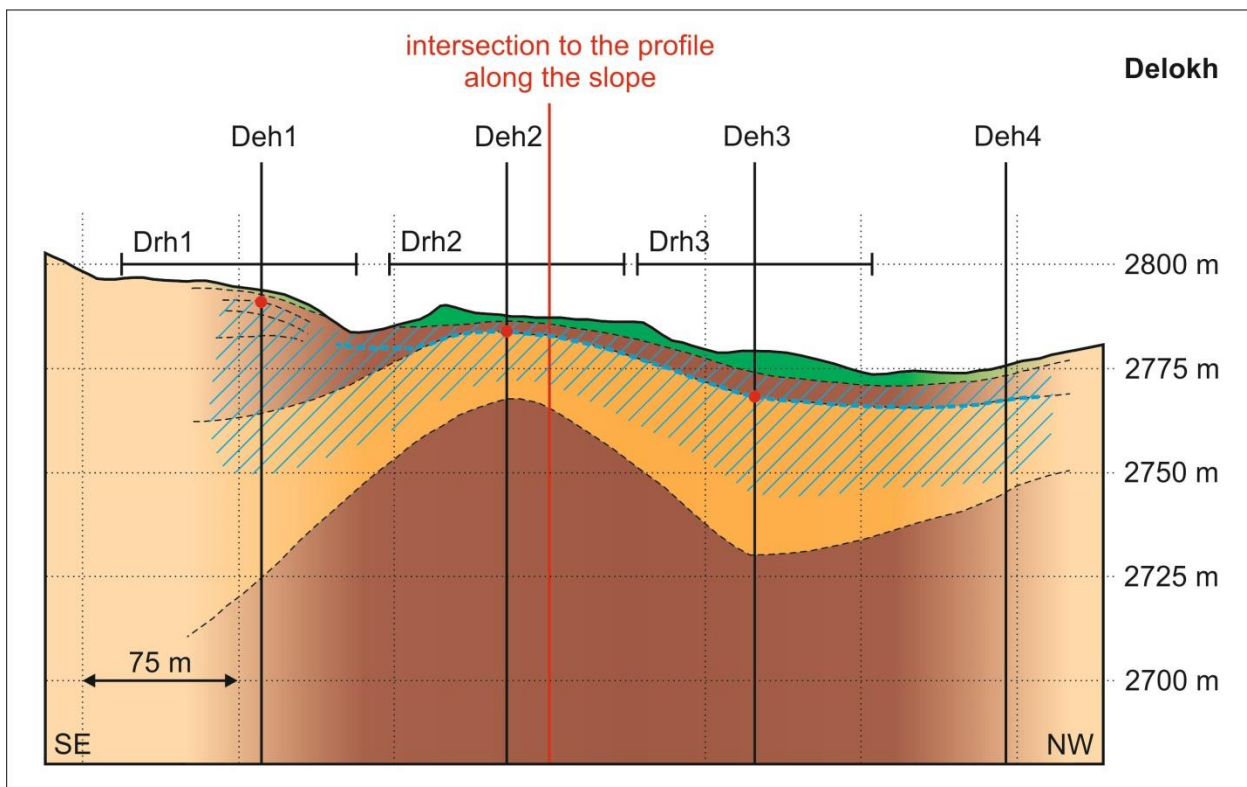


Fig. 6. Transversal cross-section (TCS) at Delokh. The red dots and the dashed blue line refer to the main sliding surface identified by both geophysical methods. The second axis is stretched for better visualization; colors are as indicated in Fig. 9.

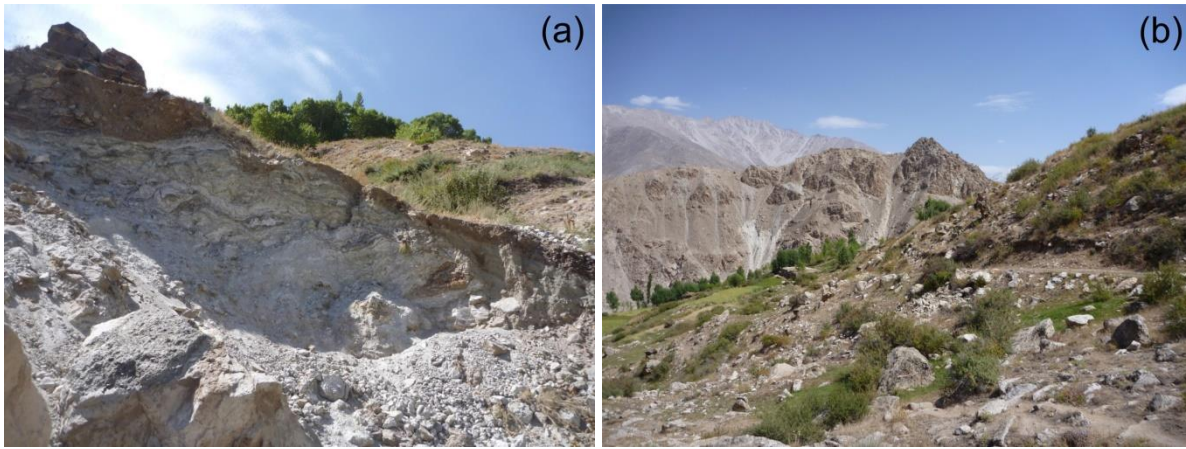


Fig. 7a-b. Dry uppermost layers in Delokh (a) extending vertically to 3-6 m; extremely coarse and uneven ground surface in Shosh (b) with boulders up to 2 m in diameter.

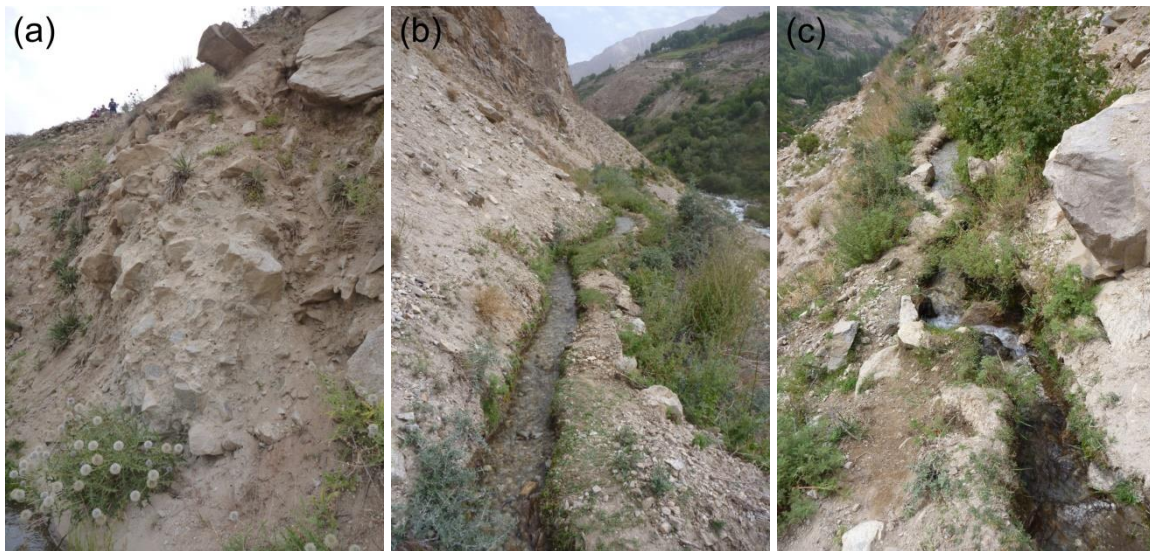


Fig. 8a-c. Example of the coarse sand layer with embedded blocks (a) in Delokh; blocks are of several decimeters in size. Non-isolated channels (b, c); both are about 40 cm wide.

Combining refraction seismics and geoelectrics data, the survey draws a realistic image that is consistent with geomorphological features that are visible at the ground surface (Fig. 6). Across the entire landslide toe (Fig. 2a, Fig. 4), very heterogeneous topsoil layers with different saturation patterns are encountered on the first meters (Fig. 7a); their heterogeneity is most likely a result of ultimate exposure to natural and anthropologic influences. The subsequent layer consists of very coarse sand with embedded gravel and blocks of various sizes that – due to its degree of decomposition and porosity – enables seepage of water to deeper horizons and, hence, appears in the geoelectric soundings as very dry (Fig. 8a). At the lower

boundaries of this unconsolidated layer, both geophysical methods detected the most prominent property changes in the form of a significant shear wave velocity increase and an abrupt resistivity decrease. Concerned depths correlate well and are shown in bold in Tab. 2 and Tab. 3.

This apparent property change can be explained by the typical layer structures of landslide deposits and by the fact that lower layers are gradually more compacted due to overlying weight. This overburden is responsible for pore volume reduction and, thus, hinders water infiltration from above. It seems, therefore, plausible that the sharp increase of conductivity is a result of seepage together with water accumulation in depths where the material becomes too dense

for further infiltration. As a consequence, the cohesion is supposed to become reduced what provides favorable conditions for the formation of sliding surfaces (cf. dashed blue line in Fig. 6). Also the shear wave velocity increase emphasizes the assumption of encountering more compacted rock material that inhibits groundwater infiltration.

Moreover, weathering plays an essential role in geophysical property patterns. Proceeding weathering processes tend to turn rock into clay-bearing material. With clay being dense and a good conductor, weathered horizons are, therefore, prone to show higher shear wave velocities along with low resistivities.

Deeper structures, as drawn in Fig. 6, are potential interpretations based on the geoelectrics survey providing information about greater depths. Here, the transition to more compacted material or bedrock lies significantly higher in the sounding Deh2 than in the other three soundings. One hypothesis explaining the deeper horizons of less compacted material west of Deh2 (i.e., below soundings Deh3-4) could be that due to pre-landslide topography the Delokh Landslide slid down rather to the west. The equally deep horizons towards the eastern side with respect to Deh2 (i.e., Deh1) might be a result of river undercutting and subsequent weathering of the gradually more exposed rock material.

Interpretations of the geophysical surveys were compared to a prior study provided by FOCUS et al. (2009) revealing several conclusive correlations. According to reports, the settlement area in Delokh was stable until the 1990s where the first reactivations of sliding surfaces within the uppermost landslide horizons and subsequent damages were detected. Almost at the same time, local solifluction and excessive water emergence from the ground were reported where the geoelectric sounding Deh2 was carried out. At this location, the water-saturated layer was

encountered much closer to the ground surface than in other areas. Furthermore, FOCUS et al. (2009) provide a map of irrigation channels crossing the inhabited zones of Delokh (Fig. 8b-c). It appears that non-isolated channels correspond well to the saturation patterns obtained by the geophysical surveys.

### 3.2. *Shosh*

The geomorphological setting in Shosh is similar to the one in Delokh – however, of a much smaller extent (Tab. 1). A post-glacial landslide slid into a topographic half-conical depression, which is bordered on its northern side by the hilltop of Lakhshik. Bearing features almost comparable to geological sagging, the landslide deposit zone is, therefore, much distorted and inhomogeneously layered what is revealed in the geoelectric soundings; no refraction seismics were carried out in Shosh.

Especially the interpretations of the geoelectric soundings along the main road through Shosh (Seh1-4) endorse a rather bipartite TCS as soundings Seh1-2 and Seh3-4, respectively, show striking differences in their resistivity patterns (Fig. 9). Except for an extremely humid and variable – most likely man-made – topsoil layer covering the totality of all four arrays (Fig. 7b), both the southern and the northern side dispose of very unevenly deep horizons of the same material group.

Starting from the southern ridge, that limits the Shosh Landslide laterally (Fig. 4), models of soundings Seh1 and Seh2 show very good correlations in terms of layering over the first 20 m from the ground surface. They reveal a classic aquifer with a thickness of a few meters above gradually more compacted sand and gravel horizons. As mentioned in the previous section, it seems likely that – because of inhibited water infiltration due to pore space reduction and clay formation as a result of weathering processes – the horizon of more compacted material behaves almost like an aquitard.

The fact that the adjacent overlying horizons are reported as very coarse and easily permeable, emphasized this assumption;

resistivities decrease here from 600-2000  $\Omega\text{m}$  to 50-300  $\Omega\text{m}$  in 4-7 m of depth (Tab. 3).

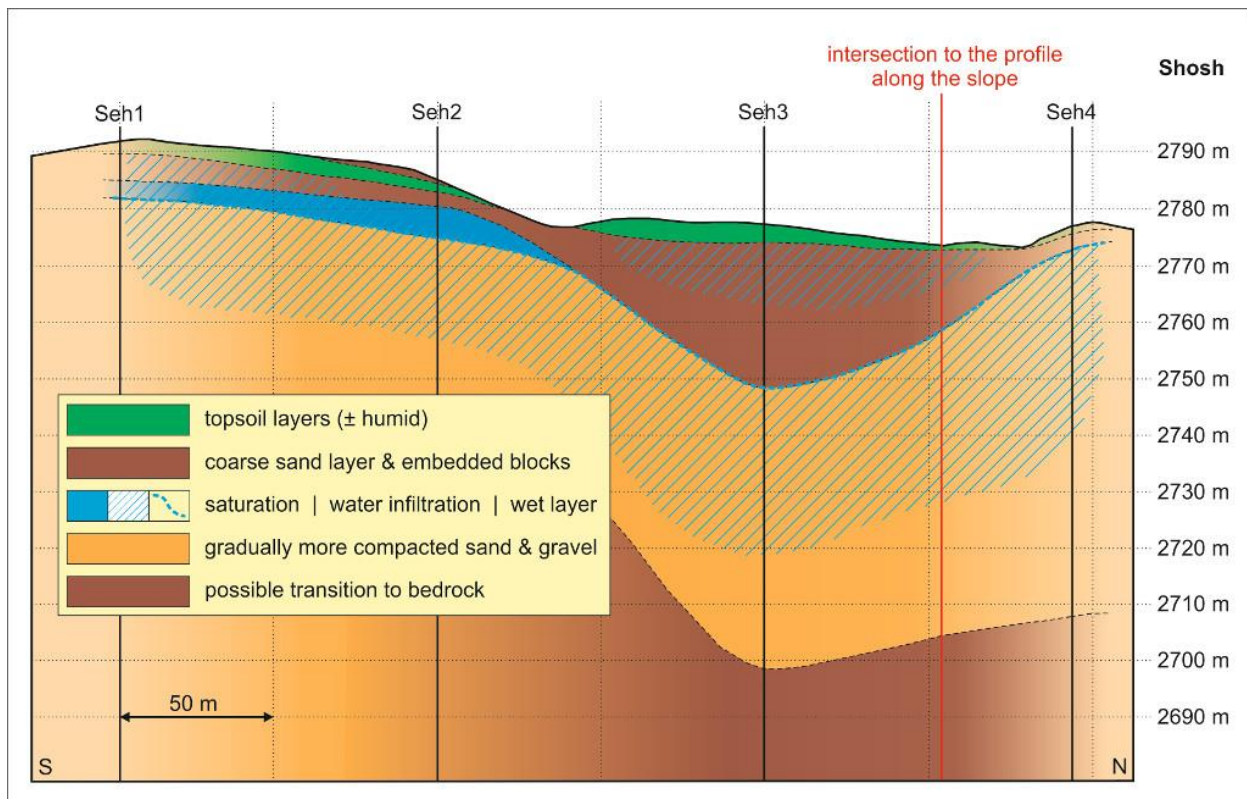


Fig. 9. Transversal cross-section (TCS) at Shosh. The dashed blue line refers to the main sliding surface identified by the geoelectrics survey. The second axis is stretched for better visualization.

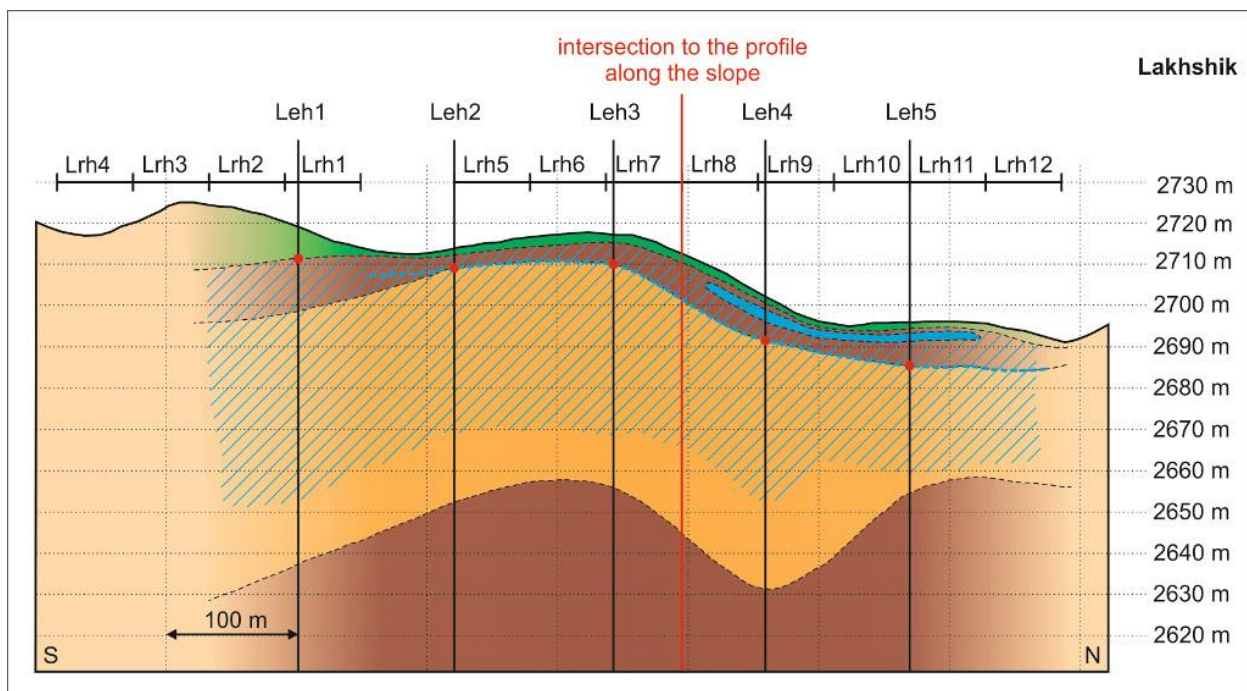


Fig. 10. Transversal cross-section (TCS) at Lakhshik. The red dots and the dashed blue line refer to the main sliding surface identified by both geophysical methods. The second axis is stretched for better visualization; colors are as indicated in Fig. 9.

The northern half of the TCS in Shosh is characterized by the pre-landslide topography that resembled a half-open cone (Fig. 4). Not only the ground surface traces the depression into which the landslide slid, but also the geoelectric soundings display a much deeper filling with coarse material and embedded blocks that remained significantly less compacted and permeable probably due to a lower overburden as the main landslide mass deviated further to the northeast towards the valley floor. Resistivities above and below the most significant layer boundary vary between the same ranges as in the southern part of the TCS (Tab. 3). However, sounding Seh3 locates the main boundary in 30 m – i.e., much deeper than its neighboring soundings – what affirms the hypothesis of a local topographic depression filled with landslide deposits. Sounding Seh4 encounters compact material in very shallow depths where the end of the entire profile joins the western extremities of the polished hilltop of Lakhshik.

The LCS of Shosh displays a uniformly parallel layering and inserts itself well to the TCS. It reveals gradually deeper water saturation towards the valley floor.

Even though the stratigraphic structures within the Shosh Landslide are more complex than within the one in Delokh, it seems plausible that reactivated sliding surfaces are likewise linked to zones of water accumulation. FOCUS et al. (2009) report secondary slides reaching and local flooding in zones where the geoelectric soundings detected the aquifer. Both phenomena coincide with the time of expanding building stock after 1995 and the construction of two irrigation channels that cross the entire landslide deposit some 20-30 m parallel to the TCS up the slope. After field investigations, it turned out that long segments of the channels are non-isolated what explains six spring crop-outs in the settlement areas and the low resistivity in the uppermost topsoil layers (Tab. 3) that decreases even to 50  $\Omega\text{m}$  at Seh2.

### 3.3. Lakhshik

The village part of Lakhshik differs in two main aspects from the other two considered locations. In geomorphological terms, on the one hand, it does not present itself as a post-glacial landslide with a traceable deposit zone, nor is the current setting explicable by one single sliding event such as in Delokh and Shosh. The slope of Lakhshik is rather characterized by steady and continuous small-scale disruptions and a general tendency of the uppermost topsoil layers progressing downslope causing damage in building stock and infrastructure. On the other hand, Lakhshik is the most inhabited of the three village parts accounting for more than a third of the settlement area of Tusion and hosting several important facilities such as schools, a medical point and the helicopter landing pad (FOCUS et al., 2009). Accounting for the higher density of settlements and the priority of distinct facilities, the slope of Lakhshik was covered by both geophysical methods over almost 1 km from south to north. Both array systems were set up along the main road that provided an altimetrically even environment and ensured proper signal transfer to the ground.

The two-layer models of the refraction seismics survey revealed an almost constant layer structure throughout the entire TCS (Fig. 10). In all individual refraction seismic profiles, shear wave velocities in the upper layer range from about 400-750 m/s in the TCS as well as in the LCS, whereas the lower layers show shear wave velocities between 900-3400 m/s (Tab. 2). The only exception is the northernmost extremity of the entire refraction seismics array system where shear wave velocities in the upper layer reach around 1000 m/s and, thus, assimilate to the velocities of deeper horizons. This latter fact could be interpreted as a lateral “fade-out” of the creeping zone where the concerned material becomes more homogeneous – i.e., where the difference between potentially unstable shallow subsurface layers and more compacted

deeper horizons becomes less significant. Refractor depths throughout all two-layer refraction seismic models vary on average between 10-15 m with some local refractor ascents almost to the ground surface and several depressions to 25 m below the ground surface.

Results with good correlation are obtained from the models of the geoelectric soundings that reveal the most significant of all resistivity changes in depths between 6-15 m within the TCS and the LCS (Tab. 3). Above these main boundaries, resistivities

range from 600-1000  $\Omega\text{m}$ ; lower horizons testify to an abrupt resistivity decrease to 150-400  $\Omega\text{m}$ . In addition to this overall conductivity pattern across the slope, the geoelectric soundings revealed an aquifer similar to the one in Shosh beneath the soundings Leh4-5. Compared to Delokh and Shosh, the geoelectrics multi-layer models show many more sublayers with different resistivity patterns within the first 2-3 m. They are supposed to be a result of more extensive land use and artificial modification of the ground surface.

Tab. 2. Array systems of the refraction seismics surveys and their results; locations of arrays are shown in Fig. 4. Single values for the depth of refractor indicate a flat layering suggested by the respective model. Bold values refer to similar depths found in the overlapping geoelectrics arrays.

Array	Length (m)	Geophone spacing (m)	Length (m)	Upper layer velocity (m/s)	Lower layer velocity (m/s)	Refractor depth (m)	Array overlap
Drh1	115.0	5.0	345	526	734	<b>6.3</b>	Deh1
Drh2	115.0	5.0		413	782	<b>5.8</b>	Deh2
Drh3	115.0	5.0		391	1066	<b>8.5</b>	Deh3
Drs4	115.0	5.0	115	580	1153	<b>0.0-18.0</b>	Des5
Drh5	57.5	2.5	230	388	1246	13.0-16.0	-
Drh6	57.5	2.5		387	1497	13.0-17.0	-
Drh7	57.5	2.5		450	1129	10.0-17.0	-
Drh8	57.5	2.5		549	959	8.0-18.0	-
Lrh1	57.5	2.5	690	437	1226	<b>2.0- 7.0</b>	Leh1
Lrh2	57.5	2.5		461	2441	4.0-25.0	-
Lrh3	57.5	2.5		584	883	0.0-11.0	-
Lrh4	57.5	2.5		415	1557	11.0-15.0	-
Lrh5	57.5	2.5		650	2365	<b>7.0-14.0</b>	Leh2
Lrh6	57.5	2.5		650	2251	2.0-20.0	-
Lrh7	57.5	2.5		750	1001	<b>4.0- 8.0</b>	Leh3
Lrh8	57.5	2.5		756	1298	5.0-24.0	-
Lrh9	57.5	2.5		679	1082	<b>3.0-19.0</b>	Leh4
Lrh10	57.5	2.5		706	1222	<b>11.0-16.0</b>	Leh5
Lrh11	57.5	2.5		1046	2125	<b>6.0-11.0</b>	Leh5
Lrh12	57.5	2.5		972	3416	3.0-14.0	-
Lrs13	57.5	2.5	115	528	1354	<b>4.0-16.0</b>	Les6-7
Lrs14	57.5	2.5		547	1858	<b>6.5</b>	Les7

Combining results from both geophysical methods, it turns out that – despite the different mass movement type – the creep in Lakhshik consists of very comparable material horizons, though with shallower thicknesses of all distinguishable material horizons. Below the rather heterogeneous topsoil layers, a continuous layer of coarse and highly permeable sand and gravel is encountered. Subsequently, models suggest more compacted material characterized by significantly higher water saturation at the top. Over the following tens of meters, conductivity decreases steadily with depth to meet the underlying compacted rock material. In contrast to the other two village parts, where bedrock is unlikely to be detected with the geophysical methods due to their limitation of reach to the underground, it seems plausible to have traced the transition to real bedrock in Lakhshik. The rock material present in Lakhshik is described to consist mainly of sand, loam and silt (FOCUS et al., 2009), which are typical for fine glacial sediments

as well as for weathered rock material. It seems, therefore, probable that deposits on the slope of Lakhshik are remnants of a glacial side moraine that – likewise – became unstable due to the lack of supporting ice masses. As the horizons bear considerably less overburden than a landslide deposit zone, even slight additional loads from increasing agglomeration and land use including irrigation might be the cause of slope instabilities.

This latter interpretation reflects one of the pre-assessments by FOCUS et al. (2009), in which slow but steady slope motion throughout the entire village part is reported since the 1990s when agglomeration increased. In 1998, after the construction of the second of the two main irrigation channels, local flooding was experienced where geoelectric soundings detected the shallowest encounters of highly saturated horizons (Leh 2-3) and several spontaneous spring crop-outs in different locations were observed.

Tab. 3. Array systems of the geoelectrics surveys and their results; locations of arrays are shown in Fig. 4. The spacing indicates the distance of the array centers. Bold values refer to similar depths found in the overlapping refraction seismics arrays.

Array	Length (m)	Spacing (m)	Length (m)	Upper layer resist. ( $\Omega$ m)	Lower layer resist. ( $\Omega$ m)	Boundary depth (m)	Array overlap
Deh1	180	120	620	2500-4000	200-800	<b>4</b>	Drh1
Deh2	220					<b>3</b>	Drh2
Deh3	220					<b>15</b>	Drh3
Deh4	80					8	-
Des5	250	80	630			<b>25</b>	Drs4
Des6	300					25	-
Seh1	220	100	770	600-2000	50-300	7	-
Seh2	250					4	-
Seh3	250					30	-
Seh4	250					2	-
Ses5	250	75	625			15	-
Ses6	300					5	-
Leh1	250	120	930	600-1000	150-400	<b>10</b>	Lrh1
Leh2	250					<b>6</b>	Lrh5
Leh3	250					<b>7</b>	Lrh7
Leh4	250					<b>15</b>	Lrh9
Leh5	200					<b>10</b>	Lrh10-11
Les6	250	120	570			<b>11</b>	Lrs13
Les7	200					<b>9</b>	Lrs13-14

After field inspection, almost all poorly isolated channel parts could be linked to heavily saturated subsoil layers and particularly to the detected aquifer that is also clearly present in the LCS as an almost perfectly slope parallel structure extending down to the end of the plateau of Lakhshik. Specifically this steep topographic step (cf. uninhabited margin northwest of Lakhshik in Fig. 4) bears the primary threat to the settlements above as the creep propagates towards an open scarp.

#### 4. Conclusions and perspectives

Despite the challenging conditions such as a remote location in a side valley in the Western Pamir and simple but functional equipment, the aim of identifying the cause of landslide activity in Tusion was successfully achieved. By the means of refraction seismics and geoelectrics an insight to the underground in the three village parts Delokh, Shosh and Lakhshik was provided in order to distinguish material properties of stratigraphic sequences, locate water-bearing horizons, identify reactivated sliding surfaces within the concerned slopes and relate the recently reported displacements across the ground surface to geological and geomorphological triggers.

The most significant observation during the model evaluation and the establishment of the cross-sections was the relation between shallow weathered horizons and water saturation. All mass movement bodies show a strong contrast of properties between the uppermost coarse, less compacted and very permeable layers and the underlying more compacted sand and gravel horizons in – roughly speaking – 10-15 m below the ground surface. This relevant contrast appears via refraction seismics modeling as refractor at which shear wave velocities significantly increase, while within models of geoelectric soundings these main layer boundaries are characterized by a sudden increase of conductivity (Fig. 5). This coincidence was finally interpreted as an interplay of two circumstances:

- Due to less overburden, weathering and land use, the uppermost layers appear coarser and allow for water infiltration to the deeper underground. Therefore, shear wave velocities are rather low and – as a result of seepage – resistivities are high. With increasing depth, also the overburden rises, causing underlying rock material to be more densely compacted and, hence, less permeable because of the lack of available pore space. Here, shear wave velocities are typically higher.
- The reason for the simultaneous increase of conductivity at lower horizons – and in particular at the interface between highly and less permeable layers –, is the process of weathering of crystalline rock and thereof consisting talus material. During this process, clay is formed, which is a good conductor.

Even though being of different geomorphological origin, both of these two major processes are present in all three mass movements: within the Delokh Landslide that is affected by river undercutting of the landslide toe; within the Shosh Landslide that resembles rather a geological sagging as it slid into a half-open topographic cone before coming temporarily to rest; and within the gravitational creep of Lakhshik that features the typical setting of an unstable ground on side moraine deposits.

Common to all three sites is the network of irrigation channels that cross the slopes, ensuring the freshwater supply to the settlements. Usually, channels are either non-isolated or in poor condition causing water to infiltrate to the underground before it accumulates at denser horizons. The process of accumulation and reduction of cohesion is believed to reactivate old sliding surfaces or form new ones. In most of the cases, the widest channels are located upslope above the settlements and, thus, favor seepage over long distances that even can be traced via vegetation patterns (Fig. 11).



Fig. 11. Non-isolated irrigation channels above settlements and their seepage patterns visible via vegetation. The picture shows the village of Sarchashma 5 km north of Khorog on the Afghan side of the Panj Valley (Fig. 1a).



Fig. 12a-c. Isolation of irrigation channels in the form of concrete pavement (a), collection and piping (b) and synthetic embedding (c).

#### 4.1. Perspectives

Although the goal of the study was met, a multitude of interplaying factors favoring landslide activity is not to be avoided or mitigated. Due to a general lack of living space in high mountainous regions, settlements are mainly located on terraces, plateaus formed by colluvial deposits, talus covered slopes or alluvial fans which – by

their nature – represent unconsolidated grounds. For this reason, relocation is rather unlikely to improve living conditions and commonly meets disapproval by local communities. Moreover – and as in the case of Tusion – settlements are subjected to expansion and development what entails more overburden as well as ground surface modification. With increasing and more developed agglomerations, freshwater

supply must be insured and, hence, irrigation channels are indispensable. In order to minimize the threat emerging from non-isolated channels, it is an absolute necessity to prevent seepage and infiltration deeper into concerned slopes. Appropriate forms of isolations might be concrete pavements, water collection in wells and distribution via pipes or synthetic embedding (Fig. 12a-c), of which some have already been implemented along the most vulnerable channel sections according to the hazard assessment by FOCUS et al. (2009).

If the slopes subjected to landslide activity in Tusion could be stabilized solely through isolation measures, remains however questionable, as movements along reactivated sliding surfaces as well as gravitational creeps are not entirely predictable and depend on a complex interplay of geological, geomorphological and geodynamical influencing factors.

### **Acknowledgments**

This work is part of the Master-Thesis of the first author and represents one of the numerous field investigations that were conducted in 2011 in the course of the project “Poverty Alleviation through Mitigation of Integrated high mountain Risk” (PAMIR) funded by the European Union (EU), co-financed by the Austrian Development Agency (ADA), implemented by the Hilfswerk International (HWI) and coordinated by the Austrian University of Natural Resources and Applied Life Sciences (BOKU), the Academy of Sciences of the Republic of Tajikistan (ANRT), Focus Humanitarian Assistance (FOCUS) and the Mountain Society Development Support Program (MSDSP) of the Aga Khan Foundation. Acknowledgments are expressed to all participants and stakeholders.

### **Contribution of the Authors**

*Gisela Domej collected the data during fieldwork for her Master-Thesis, established the main concept of the publication and primarily wrote the article. Umed Aslanov assisted in the logistic management of the field campaign, provided photographic imagery to the article and assisted with technical drawings. Anatoly Ischuk supervised the geophysical measurements as well as the interpretation of results.*

### **References**

- Bichler, A., Bobrowsky, P., Best, M., Douma, M., Hunter, J., Calvert, T., Burns, R., 2004. Three-dimensional mapping of a landslide using a multi-geophysical approach: the Quesnel Forks landslide. *Landslides*, 1(1), pp. 29-40.
- Bogoslovsky, V. A., Ogilvy, A. A., 1977. Geophysical methods for the investigation of landslides. *Geophysics*, 42(3), pp. 562-571.
- Breckle, S. W., Kleinn, E., 2011. Vegetation. In: Hauser, M. The Pamirs. Tourist Map of Gorno-Badakhshan. Gecko Maps, Zurich.
- Brooke, J. P., 1973. Geophysical investigation of a landslide near San Jose, California. *Geoexploration*, 11(2), pp. 61-73.
- Brookfield, M. E., 2000. Geological development and Phanerozoic crustal accretion in the western segment of the southern Tien Shan (Kyrgyzstan, Uzbekistan and Tajikistan). *Tectonophysics*, 328(1), pp. 1-14.
- Cummings, D., Clark, B. R., 1988. Use of seismic refraction and electrical resistivity surveys in landslide investigations. *Bulletin of the Association of Engineering Geologists*, 15(4), pp. 459-464.
- FOCUS (Focus Humanitarian Assistance), NFG (Norwegian Forestry Group), NGI (Norwegian Geotechnical Institute), MSDSP (Mountain Society Development Support Program), 2009.

- Final report on the hazard and vulnerability risk assessments conducted in the Tusyon Sub-district of the Roshtqala District in the Gorno-Badakhshan Autonomous Oblast of Tajikistan. FOCUS Humanitarian Assistance, Khorog, 19 p.
- Glade, T., Stark, P., Dikau, R., 2005. Determination of potential landslide shear plane depth using seismic refraction - a case study in Rheinhessen, Germany. *Bulletin of Engineering Geology and Environment*, 64(2), pp. 151-158.
- Google Earth, 2012. CNES/Spot Image.
- Hack, J. T., 1957. Studies of longitudinal stream profiles in Virginia and Maryland. *United States Geological Survey Professional Paper*, 294B, 59 p.
- Hack, R., 2000. Geophysics for slope stability. *Surveys in Geophysics*, 21(4), pp. 423-448.
- Havenith, H. B., Jongmans, D., Abdrakhmatov, K., Trefois, P., Delvaux, D., Torgoev, I.A., 2000. Geophysical investigations of seismically induced surface effects: case study of a landslide in the Susamyrt Valley, Kyrgyzstan. *Surveys in Geophysics*, 21(4), pp. 349-369.
- Havenith, H. B., Torgoev, I., Ischuk, A., 2018. Integrated Geophysical-Geological 3D Model of the Right-Bank Slope Downstream from the Rogun Dam Construction Site, Tajikistan. *International Journal of Geophysics*, 2018(ID 1641789), 16 p.
- INTERPEX, 2008a. IXRefraX Instruction Manual (version 1.2). Interpex Limited, Golden, 73 p.
- INTERPEX, 2008b. IX1D Instruction Manual (version 1.0). Interpex Limited, Golden, 67 p.
- Jongmans, D., Garambois, S., 2007. Geophysical investigation of landslides: a review. *Bulletin Société Géologique de France*, 178(2), pp. 101-112.
- Karapetov, S. S., Sonin, I. I., Khain, V. Y., 1975. On some important features of structure and evolution of the Afghan-Pamir segment of the Alpine fold belt. *Bulletin of the Moscow University of Geology*, 3, pp. 38-46. (in Russian)
- Konagai, K., Numada, M., Zafeirakos, A., Johansson, J., Sadr, A., Katagiri, T., 2005. An example of landslide-inflicted damage to tunnel in the 2004 Mid-Niigata prefecture earthquake. *Landslide*, 2(2), pp. 159-163.
- Kordonskaya, N. W., Shebalin, N. W., 1977. New strong earthquake catalog for the territory of the USSR from the past to the year 1975. Nauka, Moscow, 536 p. (in Russian)
- Kreutzmann, H., 2011a. Pamir ecology: glaciers and high mountain desert. In: Hauser, M. *The Pamirs. Tourist Map of Gorno-Badakhshan*. Gecko Maps, Zurich.
- Kreutzmann, H., 2011b. Introduction. In: Hauser, M. *The Pamirs. Tourist Map of Gorno-Badakhshan*. Gecko Maps, Zurich.
- Mauritsch, H. J., Seiberl, W., Arndt, R., Römer, A., Schneiderbauer, K., Sendlhofer, G. P., 2000. Geophysical investigations of large landslides in the Carnic Region of southern Austria. *Engineering Geology*, 56(3-4), pp. 373-388.
- Searle, M., 2008. Geology of Tajikistan. In: Middleton, R., Thomas, H. *Tajikistan and the High Pamirs*. Odyssey Books & Guides, Hong Kong, pp. 236-240.
- Singh, R. P., Dubey, C. S., Singh, S. K., Shukla, D. P., Mishra, B. K., Tajbakhsh, M., Ningthoujam, P. S., Sarma, M., Singh N., 2012. A new slope mass rating in mountainous terrain, Jammu and Kashmir Himalayas: application of geophysical technique in slope stability studies. *Landslides*, 10(3), pp. 255-265.
- Slavin, V. I., 1976. *Tectonics of Afghanistan*. Nedra, Moscow, 204 p. (in Russian)
- Strom, A., Abdrakhmatov, K., 2018. *Rockslides and Rock Avalanches of Central Asia - Distribution, Morphology, and Internal Structure*. Elsevier, Oxford, 458 p.